

Composition gradient as a source of pinning in Nb–Ti and NbTa–Ti superconductors

This article has been downloaded from IOPscience. Please scroll down to see the full text article.

2007 J. Phys.: Condens. Matter 19 446204

(<http://iopscience.iop.org/0953-8984/19/44/446204>)

View [the table of contents for this issue](#), or go to the [journal homepage](#) for more

Download details:

IP Address: 129.252.86.83

The article was downloaded on 29/05/2010 at 06:30

Please note that [terms and conditions apply](#).

Composition gradient as a source of pinning in Nb–Ti and NbTa–Ti superconductors

Cristina Bormio-Nunes¹, Maria José R Sandim¹ and L Ghivelder²

¹ Escola de Engenharia de Lorena, Universidade de São Paulo, CP116, Lorena, SP 12602-860, Brazil

² Instituto de Física, Universidade Federal do Rio de Janeiro, CP 68528, Rio de Janeiro, RJ 21941-972, Brazil

Received 3 July 2007, in final form 27 September 2007

Published 16 October 2007

Online at stacks.iop.org/JPhysCM/19/446204

Abstract

Superconducting Nb–Ti and NbTa–Ti wires produced by solid-state diffusion were studied, correlating microstructural and transport properties. The most interesting result is that the diffusion layer sharp composition variation is an important source of pinning in these materials. Within this scenario, we suggest that the source of pinning centers in conventional NbTi wires should be re-examined, since the α -Ti precipitation creates a Nb gradient composition around it. We propose that in conventional superconducting wires there are actually two kinds of strong pinning centers. One is the well-known α -Ti normal interface and the new one now identified is the composition gradient around α -Ti precipitates.

1. Introduction

Identifying pinning centers and pinning mechanisms is of major importance for achieving higher critical currents in superconducting wires. In the early 1980s several flux line pinning (FLP) studies were made on the Nb–Ti system, considering the pinning produced by grain boundaries and small precipitates [1, 2]. At that time, the defect microstructure of the optimized Nb–Ti conventional wires was often thought of as too complex for basic FLP studies. The detailed knowledge of the microstructure of the optimized Nb–Ti conventional wires (without artificial pinning centers) was achieved only after 1989 [3]. The defect structure in optimized Nb–Ti wires was found to be made up of very thin (1–4 nm) α -Ti ribbons separated by 2–10 nm and with lengths extending to 1000–2000 nm [4]. Up to now, α -Ti precipitates have been considered as the most relevant pinning sources in Nb–Ti wires, and many FLP mechanisms have been proposed to explain the flux line anchoring by them. The most important FLP mechanisms are the following: *core pinning* and *magnetic pinning*. The *core pinning* mechanism supposes that the flux line sits on the α -Ti precipitate, saving the energy of the core nucleation and therefore lowering the energy of the system [5]. The

magnetic pinning mechanism assumes that the presence of the precipitate changes the field and current distribution around the flux line and thus introduces a position dependence of the free energy required to rise to the so-called magnetic interaction. More specifically, the flux lines are subjected to an attractive force exerted by the planar interface of the α -Ti ribbons and this force opposes the driving force on the flux lines [6]. Still within the scope of the magnetic interaction, there is yet another model that considers the electric nature (resistive behavior) of the pinning centers [7]. In addition to magnetic and core pinning, a different point of view was introduced by Lazarev and collaborators, which resulted from observations of the Nb–Ti microstructure using field ion microscopy [8, 9]. Their work highlights the existence of the composition variation close to the α -Ti precipitate. This finding was later confirmed using high resolution field emission microscopy [10]. They suggested that the high current-carrying capacities of Nb–Ti alloys are due to the presence of phases with composition close to pure Nb. These phases precipitate as a result of thermomechanical treatments and develop a three-dimensional lattice of inclusions, which are the relevant current-carrying paths in conventional Nb–Ti wires. This scenario agrees with studies on Nb–Ti and NbTaTi wires produced from pure Nb and/or Nb–20%Ta (% in mass) and pure Ti by solid-state diffusion [11–13]. The alloy that has enhanced superconducting properties when compared with pure Nb and Nb–Ta is formed throughout the diffusion between Nb and Ti or Nb–20%Ta and Ti. The sharpness of the diffusion layer composition profile in this kind of material is an important source of pinning [12, 13]. This result calls attention to the importance of the Ti and Nb composition gradient developed also in the vicinity of α -Ti precipitates, as Lazarev’s works suggest [8–10]. Our conclusions are based on microstructure and transport measurements for Nb–Ti and NbTa–Ti superconducting wires, produced by diffusion in the solid state.

It is important to highlight that it is not our objective to compare the performance of our APC NbTi wires produced by solid-state diffusion with that of conventional NbTi wires. This is not possible because the density of pins in the APC wires is very low since their sizes are on the micrometer scale, resulting in critical current densities of about 1×10^4 A cm⁻² at 2 T. On the other hand, conventional NbTi wires have pinning centers on the nanometer scale, and therefore the critical current density is of the order of 6×10^5 A cm⁻² at 2 T.

2. Experimental procedure

Nb–Ti was manufactured as a multifilament wire with 125 monofilaments dispersed in a Cu–10%Ni (% in mass) normal matrix and placed around a Cu nucleus. The monofilament is formed by 84 subfilaments (Ti bar inside a Nb) positioned around a Nb bar. More details of the wire manufacture and superconducting properties are given elsewhere [11] and [12]. In the present work we present the microstructure, diffusion layer composition and critical current density results for the Nb–Ti multifilament wire at 1.43 mm diameter for two conditions: non-heat-treated (NHT) and heat-treated wires (HT). The former corresponds to a wire produced without applying heat treatments in order to obtain the diffusion layer. The HT wires come from the NHT wire at 1.43 mm diameter that was heat treated for 2 h at 873, 923 and 973 K. Nevertheless, both NHT and HT wires received heat treatments during the wire manufacture intended for mechanical property improvements.

The main characteristics of the superconducting Nb–Ti–Ta wire are the following: it is a monofilament wire that corresponds to the subfilament in the case of the Nb–Ti wire already described. But in this case the Nb–20%Ta alloy tube substitutes the Nb tube and an external Cu tube substitutes the Cu–Ni alloy tube. The monofilament Cu + Nb–20%Ta + Ti was swaged and drawn down to the diameter of 0.64 mm. A diffusion layer was developed during the processing of the wire, but this layer thickness was strongly reduced by the deformation

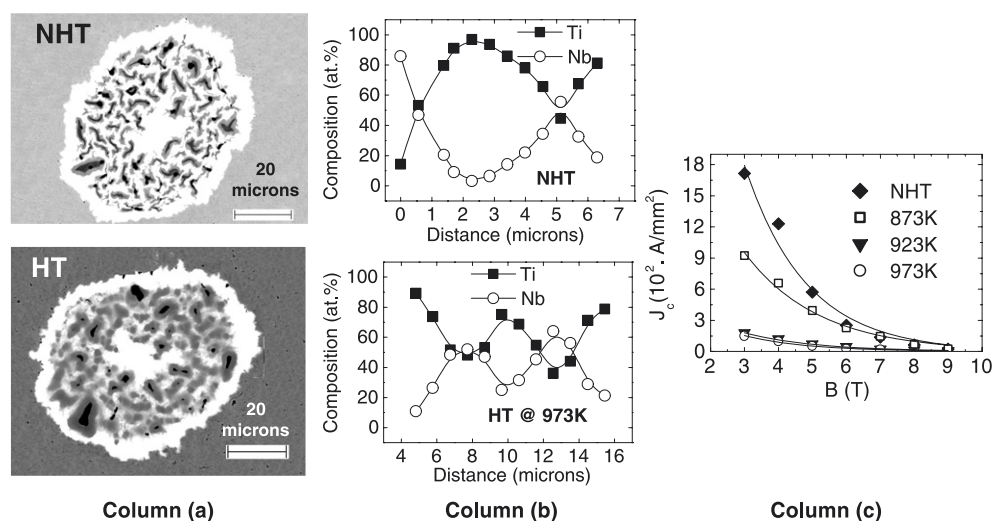


Figure 1. Results on Nb–Ti multifilament wire at 1.43 mm diameter and NHT and HT conditions: column (a) micrographs of one typical monofilament of the wire NHT and HT (973 K—2 h); column (b) Ti and Nb composition profile of one typical subfilament and column (c) J_c versus B curves.

process [13]. At 0.64 mm diameter heat treatments were made for 120 h at temperatures of 973, 1023 and 1073 K, and the related diffusion layer average thicknesses are 7, 15 and 20 μm .

For both wires, the heat treatments applied during their manufacture were always at $T \geq 973$ K for 1–4 h and subsequently the wires were immediately quenched. The purposes of the heat treatments were to retain the β -phase and to recover/recrystallize the composite material, in order to improve the ductility. Both, Nb + Ti and NbTa + Ti wires could be easily drawn after these heat treatments [12, 13]. The critical current density was calculated dividing the critical current by the transverse area of the diffusion layer estimated from SEM pictures and using image analysis.

3. Results and discussion

In column (a) of figure 1 we show micrographs of only one typical monofilament, of the Nb–Ti wire at 1.43 mm diameter in NHT conditions and HT at 973 K. We observe that the NHT subfilaments present a small diffusion layer (gray color) produced by initial heat treatment during the wire manufacture. On the other hand, the HT wire presents most of the subfilaments completely reacted (gray regions). The black regions correspond to pure Ti and the white regions to pure Nb. In column (b) we display the composition profile of one subfilament (average size of 7 μm) at the specific conditions shown in column (a). The increase of heat treatment temperature enhances the high field superconducting volume phase and partial composition homogenization is achieved. In addition, there is a decrease of the Nb phase thickness. Finally, column (c) shows the critical current density for the NHT and HT wires.

The cross section of the NbTa–Ti monofilament heat treated at 1023 K appears in figure 2(a). Figures 2(b) and (c) show the composition profiles and the related plots of J_c versus $\mu_0 H$. In this case the heat treatment temperatures and time were not enough to totally consume the Ti. Nevertheless, we observed the same trend in the J_c curves as in Nb–Ti wire previously described, namely, as the heat treatment temperature increases, J_c decreases, despite the growth of the high field superconducting area and Nb–Ta thickness decrease.

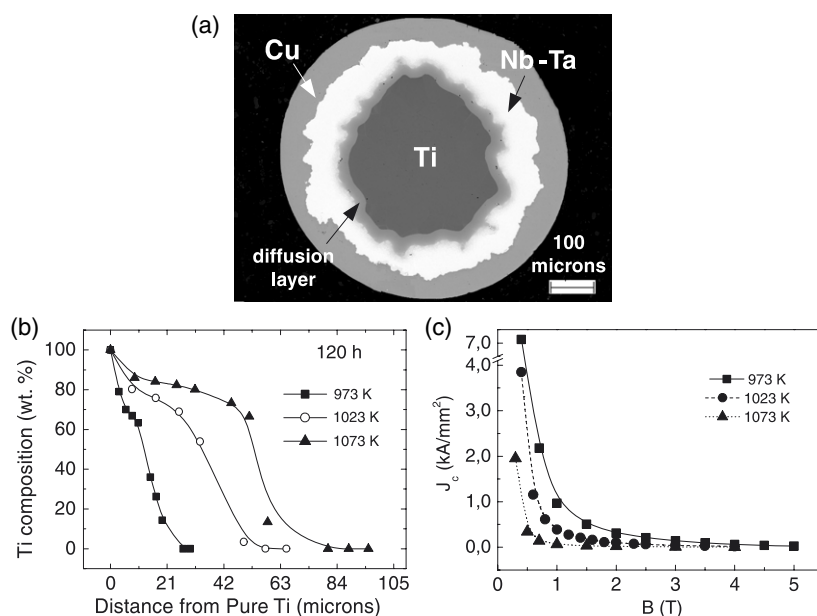


Figure 2. Results on Nb–Ti–Ta wire at 0.64 mm diameter: (a) micrograph of monofilament cross section HT at 1023 K for 120 h; (b) Ti composition profile for each HT temperature and column (c) J_c versus B respective curves.

The interface between pure Ti and the diffusion layer is also a source of pinning in both Nb–Ti and Nb–Ti–Ta wires. However, this pinning center is relevant only for the Nb–Ti NHT wire, due to the large interface that exists between pure Ti and the diffusion layer (figure 1(a)—NHT wire), which almost disappears upon heat treatment. In the case of the NbTa–Ti the Ti–diffusion layer interface change is very small. The reduction in this interface area is only 4% when comparing wires treated at 973 and 1023 K, and 2% from 1023 to 1073 K. Therefore as the homogenization of the diffusion layer is achieved there is a decrease of J_c , as can be observed in a constant composition range in figure 2(b) at 1073 K.

The presence of α -Ti precipitates as the main source of pinning in these materials can be safely rejected, since the heat treatments applied during wire manufacture at $T \geq 973$ K followed by water quenching eliminate them. Only for alloys with 85% Ti or higher is the presence of α -Ti possible (Nb + Ti system) for this temperature [14]. However, these high Ti alloys have lower critical temperatures, $T_c < 5$ K [15]. We believe that these successive heat treatments were also sufficient to annihilate most of the dislocations induced by the wire deformation. In addition, the presence of dislocations would improve J_c for higher fields, which was not observed. Neal *et al* [16] showed very clearly that a heat treatment of 1 h at 873 K in a wire of Nb–44%Ti (% in mass) and with an area reduction of 5×10^4 , presented a very low current-carrying capacity and virtually constant Lorentz force for fields up to 6 T. The same conclusions are valid for the NbTa + Ti wire since the β -phase boundary temperatures in the ternary phase diagram and critical temperatures of the ternary and binary alloys are similar for comparable Ti contents [16, 17].

Figure 3 shows the variation of the critical field B_{c2} of the NbTa–Ti wire for the three heat treatment conditions. It can be observed that the highest value of B_{c2} corresponds also to wire that presents the highest value of J_c . This result indicates that this wire with a very sharp

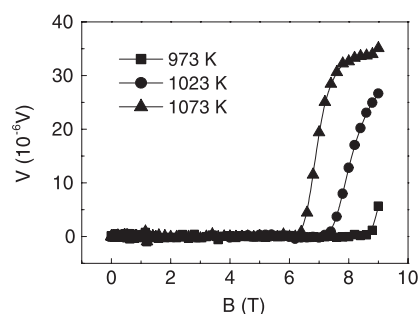


Figure 3. Upper critical field B_{c2} measurement curves for Nb–Ti–Ta wire at 4.2 K.

composition profile corresponds to the optimized condition of the diffusion layer. A complete study of the transport and magnetic properties of this wire will be published elsewhere.

Finally, we address the question of which type of flux line pinning (FLP) occurs in this kind of material. Examining the magnetic pinning, this mechanism is relevant only at the diffusion layer border (superconducting–normal interfaces) in the positions where the flux line has an appreciable part of the length parallel to this interface. It is easier to visualize this in the NbTa + Ti wire (see figure 2(a)). However, as already discussed, this interface was not relevant to the change in J_c and consequently is not a significant source of FLP. On the other hand, the flux lines formed on the diffusion layer do not have a fixed core size ξ ($\xi = (\phi_0/2\pi B_{c2})^{1/2}$, $\phi_0 = 2 \times 10^{-15}$ Wb), because B_{c2} varies with composition. The flux line core has a larger diameter near the diffusion layer interfaces, close to the pure Nb (NbTa) and Ti (B_{c2} values are smaller). At the layer central part the diameter is smaller, because B_{c2} is higher. This variation of the core energy along the flux line length gives rise to the flux pinning force. In this sense, we may conclude that the major flux pinning mechanism is of a core pinning type and that it is directly linked to the sharp variation of the composition of the diffusion layer in the central part of the layer.

4. Conclusions

From results on both Nb–Ti and Nb–Ti Ta wires we found that a sharp variation of the diffusion layer composition is an important source of flux pinning in this kind of material. This important finding changes significantly the understanding of flux line pinning in the long known Nb–Ti superconductors. It is evident that a re-investigation of where the effective flux pinning centers are in conventional NbTi wires is necessary. The Ti and Nb gradient composition caused by the α -Ti precipitation has to be considered in flux pinning analysis, and consequently it is important for J_c optimization as well as the specific α -Ti normal interfaces. We claim that the Ti and Nb gradient is also a major source of pinning, in addition to the normal interfaces of α -Ti precipitates. This finding explains why the maximum in pinning forces curves occurs at different fields in conventional wires ($\mu_0 H \approx 5$ T) [3] and in artificial pinning center wires with Nb pinning ($\mu_0 H \approx 3$ T) [18]. In Nb artificial pinning center wires, the pinning is due only to the normal interfaces of pure Nb.

Acknowledgments

This work was supported by FAPESP grants under number 97/06357-3 and 97/11113-6. FAPERJ and CNPq supported LG.

References

- [1] Panek M, Pattanayak D, Meier-Hermer R and Kuepfer H 1983 *J. Appl. Phys.* **54** 7083
- [2] Larbalestier D C and West A W 1984 *Acta Metall.* **32** 1871
- [3] Meingast C, Lee P J and Larbalestier D C 1989 *J. Appl. Phys.* **66** 5962
- [4] Lee P J 1999 *Wiley Encyclopedia of Electrical and Electronic Engineering* vol 21 (New York: Wiley) pp 75–87
- [5] Meingast C and Larbalestier D C 1989 *J. Appl. Phys.* **66** 5971
- [6] Slezov V V, Chernyi O V and Davidov L N 2005 *Supercond. Sci. Technol.* **18** 747
- [7] Cooley L D, Lee P J and Larbalestier D C 1996 *Phys. Rev. B* **53** 6638
- [8] Lazarev B G, Khorenko V K, Kornienko L A, Krivko A I, Matsakova A A and Ovcharenko O N 1964 *Sov. Phys.—JETP* **18** 1417
- [9] Garber R J, Lazarev B G, Lazareva L S, Mikkailovskii I M and Sidorenko N N 1973 *Sov. Phys.—JETP* **36** 718
- [10] Lazarev B G, Ksenofontov V A, Mikkailovskii I M and Velikodnaya O A 1998 *Low Temp. Phys.* **24** 205
- [11] Bormio-Nunes C, Nunes C A, Tirelli M A, Edwards E R and Porto F S A 2003 *Supercond. Sci. Technol.* **16** 521
- [12] Bormio-Nunes C, Sandim M J R, Edwards E R and Ghivelder L 2006 *Supercond. Sci. Technol.* **19** 1063
- [13] Bormio-Nunes C, Gomes P M N, Tirelli M A and Ghivelder L 2005 *J. Appl. Phys.* **98** 043907
- [14] Na L and Warnes W H 2001 *IEEE Trans. Appl. Supercond.* **11** 3800
- [15] Collings E W 1983 *A Source Book of Titanium Alloy Superconductivity* (New York: Plenum) chapter 7, pp 213–324
- [16] Neal D F, Barber A C, Woolcock A and Gidley J A 1971 *Acta Metall.* **19** 143
- [17] Suenaga M and Ralls K M 1969 *J. Appl. Phys.* **1** 4457
- [18] Heussner R W, Bormio-Nunes C, Cooley L D and Larbalestier D C 1997 *IEEE Trans. Appl. Supercond.* **7** 1142